



One man's trash is another man's treasure—the effect of bacteria on phytoplankton–zooplankton interactions in chemostat systems

M. Raatz ^{1,*} S. Schällicke,¹ M. Sieber,² A. Wacker,¹ U. Gaedke ¹

¹University of Potsdam, Potsdam, Brandenburg, Germany

²Max-Planck Institute for Evolutionary Biology, Plön, Schleswig-Holstein, Germany

Abstract

Chemostat experiments are employed to study predator–prey and other trophic interactions, frequently using phytoplankton–zooplankton systems. These experiments often use population dynamics as fingerprints of ecological and evolutionary processes, assuming that the contributions of all major actors to these dynamics are known. However, bacteria are often neglected although they are frequently present. We argue that even without external carbon input bacteria may affect the experimental outcomes depending on experimental conditions and the physiological traits of bacteria, phytoplankton, and zooplankton. Using a static carbon flux model and a dynamic simulation model, we predict the minimum and maximum impact of bacteria on phytoplankton–zooplankton population dynamics. Under bacteria-suppressing conditions, we find that the effect of bacteria is indeed negligible and their omission justified. Under bacteria-favoring conditions, however, bacteria may strongly affect average biomasses of phytoplankton and zooplankton. The population dynamics may become highly complex, which may result in wrong interpretations when inferring processes (e.g., trait changes) from population dynamic patterns without considering bacteria. We provide suggestions to reduce the bacterial impact experimentally. Besides optimizing experimental conditions (e.g., the dilution rate) the appropriate choice of the zooplankton predator is decisive. Counterintuitively, bacteria have a larger impact if the predator is not bacterivorous as high bacterial biomasses and complex population dynamics arise via competition for nutrients with the phytoplankton. Only at least partial bacterivory minimizes the impact of bacteria. Our results help to improve the design of chemostat experiments and their interpretation, and advance the study of ecological and evolutionary processes in aquatic food webs.

Highly controllable and easy to handle laboratory experimental approaches are a useful tool to understand complex trophic interactions in natural systems. A prominent representative of these are phytoplankton–zooplankton chemostat experiments which have proven themselves in multiple studies of basic ecological and evolutionary concepts, see e.g. Novick and Szilard (1950); Fussmann et al. (2000); Yoshida et al. (2003); Becks et al. (2012); Hiltunen et al. (2013); Declerck et al. (2015). Aside from biomass levels, these experiments often focus on patterns in population dynamics, which are fingerprints of interactions between the organisms. While they are undoubtedly able to provide proof-of-concept-like dynamics, chemostat experiments occasionally lack reproducibility, with unexpected experimental runs often not being published, and inference from individual chemostat experiments may be difficult (Bengfort et al. 2017). We hypothesize

that bacteria may be one cause of such experimental irregularities.

In numerous chemostat experiments, bacteria are an unwanted but often unavoidable and inherent part of the system. While phytoplankton cultures may be run axenically, most zooplankton cultures contain at least parts of the microbiome of the animals (Ishino et al. 2012; Seah et al. 2017). Due to the usually long duration of chemostat experiments also an unintended introduction of bacteria may eventually occur. Phytoplankton exudation and zooplankton excretion drive production of dissolved and particulate organic carbon, providing resources for these bacteria even without an organic carbon source in the growth medium (Vadstein et al. 2003). Bacteria may hamper algal growth by competition for nutrients (Bratbak and Thingstad 1985) and bacterivory can constitute a substantial portion of zooplankton production (Starkweather et al. 1979; Arndt 1993; Ooms-Wilms 1997).

Nevertheless, bacteria are often neglected in chemostat studies. Motivated by earlier experimental investigations (Starkweather et al. 1979; Aoki and Hino 1996; Hino

*Correspondence: michael.raatz@uni-potsdam.de

Additional Supporting Information may be found in the online version of this article.

et al. 1997), we challenge this omission and study under which conditions bacteria can substantially influence phytoplankton growth and contribute to zooplankton production, and thereby affect the shape of predator–prey cycles in a typical chemostat experiment.

First, we show that already a simple carbon flux model based on a few assumptions without population dynamics predicts that the impact of bacteria may become large. We therefore include a carefully parametrized microbial loop into a standard phytoplankton–zooplankton chemostat model (Fussmann et al. 2000) (Fig. 1) and study changes in mean biomasses and population dynamics. We analyze how the response of the system to the presence of bacteria depends on experimental conditions, whether the physiological traits of bacteria, phytoplankton, and zooplankton favor or suppress bacteria, and how well the zooplankton is able to ingest the bacteria, i.e., its degree of bacterivory. The experimental conditions determine the relative importance of nutrient inflow and losses of nutrients and organisms due to washout on the one hand vs. the internal recycling of nutrients and grazing-induced mortality on the other hand. The physiological traits of phytoplankton and zooplankton determine the rate at which organic carbon is produced and the fierceness of the competition for limiting nutrients between algae and bacteria. The degree of bacterivory of the zooplankton determines the grazing pressure on the bacteria. Experimental conditions, physiology, and degree of bacterivory thus define the conditions under which bacteria may or may not thrive and impact the system.

To sharpen the focus of chemostat experiments on the phytoplankton–zooplankton interaction, the question arises how the unwanted but unavoidable effect of bacteria can be minimized. One intriguing strategy to follow could be choosing

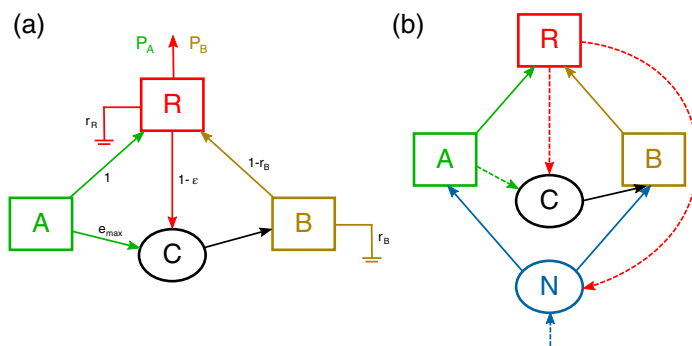


Fig. 1. Food web sketches with the limiting resource nitrogen (N), organic carbon pool (C), algae (A), bacteria (B), and rotifers (R). **(a)** Static carbon flux model with parameters as used in Eq. 1. One unit of algal production directly sustains predator excretion, respiration and production (P_A), but also entails additional carbon. These exudates fuel a pool of organic carbon that allows for bacterial production. This bacterial production per unit algal production also increases predator production (P_B). Respiratory losses are depicted by earth ground symbols. **(b)** Dynamic phytoplankton–zooplankton chemostat model as given by Eq. 2. Here, solid arrows represent consumption, substance flows are shown in dashed arrows and respiratory fluxes are omitted for clarity.

zooplankton species with a low degree of bacterivory, assuming that non-ingested bacteria would hardly affect the system. Thus, rotifers, which are often less bacterivorous than ciliates (Arndt 1993), may be favored for phytoplankton–zooplankton chemostat experiments. Instead, we find that the effect of bacteria is low at high degrees of bacterivory. By considering bacteria as inherent actors in phytoplankton–zooplankton experiments, we are able to predict conditions when the effect of bacteria is large and provide means to minimize it.

Materials and procedures

We employ two models to study the effect of bacteria on phytoplankton–zooplankton interactions. We start with a simple static carbon flux model (Fig. 1a) to estimate how much predator production may result from bacterial production and how this depends on algal exudation, predator excretion, and bacterial growth efficiency. Then, we develop a dynamic chemostat model that provides insights into the mean biomasses and population dynamics of all species, which comes at the costs of requiring more assumptions (Fig. 1b).

In both models, the rate of organic carbon production depends on the physiological parameters for maximal algal exudation e_{\max} and predator excretion $(1 - \epsilon)$, ϵ being the predator assimilation efficiency. How efficiently this carbon pool can be used by the bacteria is set by their growth efficiency $(1 - r_B)$, with the bacterial respiration r_B . Bacteria are suppressed by low carbon supply, which occurs at low algal exudation and low predator excretion, and inefficient use of that carbon by the bacteria. Bacteria are favored by high carbon supply, i.e., at high algal exudation, predator excretion, and bacterial growth efficiency. Using the lower and upper end of the broad ranges of published values for these parameters (Table 1, Supporting Information Appendix 1) we construct a minimum and a maximum impact scenario of conditions suppressing or favoring bacteria, respectively.

Suppressing conditions

$$e_{\max} = 0.2 \quad (1 - \epsilon) = 0.3 \quad (1 - r_B) = 0.3$$

Favoring conditions

$$e_{\max} = 0.4 \quad (1 - \epsilon) = 0.6 \quad (1 - r_B) = 0.6$$

In the following, we investigate the effect of bacteria by employing these two extreme scenarios, which account for the great variability of observed bacterial growth conditions. We focus on typical chemostat experiments with obligatory autotrophic algae. We do not include bacterial toxicity, which might become important at high bacterial densities that are less likely to occur without additional carbon sources. Such high densities of toxic bacteria would result in predator extinction and the chemostat experiments would be stopped.

Static carbon flux model

A first estimate of the effect of bacteria for the two extreme cases of suppressing and favoring conditions for bacterial growth can be obtained from a static model of the carbon

Table 1. Parameters and their biological meaning. Ranges are given for parameters that were varied within this study. Parameter values are either estimated from unpublished chemostat runs (Guntram Weithoff, Svenja Schällicke, pers. comm.) or taken from literature. See also the description of parameter choice in Supporting Information Appendix 1.

| Parameter | Biological meaning | Value | Reference |
|-----------------|--|--|--|
| e_{\max} | Maximum carbon exudation of algae | 0.2 – 0.4 | Varied (Baines and Pace 1991) |
| e_{\min} | Minimum carbon exudation of algae | 0.1 | Varied (Baines and Pace 1991) |
| r_B | Carbon respiration by bacteria | 0.4 – 0.7 | Varied (del Giorgio and Cole 1998) |
| r_R | Carbon respiration by rotifers | 0.5 | Humphreys (1979) |
| ε | Carbon assimilation efficiency of rotifers | 0.4 – 0.7 | Varied (Straille 1997) |
| δ | Chemostat dilution rate | 0.07 – 0.7 d ⁻¹ | Varied within standard experimental ranges, see e.g., Vadstein et al. (2003) or Fussmann et al. (2000) |
| N_I | Inflow resource concentration | 160 $\mu\text{molN L}^{-1}$ | Set to standard experimental conditions, see e.g., Becks et al. (2010) |
| $\omega_{A, N}$ | N content in an algal cell | $4.6 \times 10^{-8} \mu\text{molN}$ | Estimated from unpublished data, G. Weithoff |
| $\omega_{B, N}$ | N content in a bacterial cell | $8.8 \times 10^{-10} \mu\text{molN}$ | From $\omega_{B, C}$ with C:N=5.65 (Vrede et al. 2002) |
| $\omega_{R, N}$ | N content in a rotifer | $1.2 \times 10^{-3} \mu\text{molN}$ | Estimated from unpublished data, G. Weithoff |
| $\omega_{A, C}$ | C content in an algal cell | $5 \times 10^{-7} \mu\text{molC} \triangleq 6 \text{ pgC}$ | Estimated from unpublished data, G. Weithoff |
| $\omega_{B, C}$ | C content in a bacterial cell | $5 \times 10^{-9} \mu\text{molC} \triangleq 60 \text{ fgC}$ | Set to 1/100 of $\omega_{A, C}$ in agreement with Vrede et al. (2002) |
| $\omega_{R, C}$ | C content in a rotifer | $6.7 \times 10^{-3} \mu\text{molC} \triangleq 80 \text{ ngC}$ | From $\omega_{R, N}$ with C:N=5.6 (Jensen et al. 2006), in agreement with Dumont et al. (1975) |
| β_A | Maximum algal growth rate | 1.9 d ⁻¹ | Estimated from unpublished data, S. Schällicke |
| β_B | Maximum bacterial growth rate | 1 d ⁻¹ | Morris and Lewis (1992) |
| G | Rotifer maximum ingestion rate | $3.6 \text{ d}^{-1} \triangleq 288 \text{ ngC d}^{-1}$ | Rothhaupt (1990) |
| H_A | Algal half-saturation | $49 \mu\text{molN L}^{-1}$ | Estimated from unpublished data, S. Schällicke |
| $H_{B, N}$ | Bacterial half-saturation for nitrogen | $4.9 \mu\text{molN L}^{-1}$ | Set to 1/10 of the algal half-saturation |
| $H_{B, C}$ | Bacterial half-saturation for carbon | $0.83 \mu\text{molC L}^{-1}$ | Tittel et al. (2012) |
| H_R | Rotifer half-saturation | $195 \mu\text{molC L}^{-1} \triangleq 2.34 \text{ mgC L}^{-1}$ | Set, in approximate agreement with Fussmann et al. (2000) |
| p_B | Degree of bacterivory of the rotifer | 0.01 – 1 | Varied |

fluxes between algae, bacteria, and predators. We constructed a model similar to those presented by Anderson and Ducklow (2001) and Gaedke et al. (2002) to compute the predator production that originates from bacterial production for different physiological parameters, i.e., bacteria-suppressing or -favoring conditions (Fig. 1a). We assume a steady state for all species. This translates to maximal algal exudation, as nitrogen limitation is high. Algal exudation is assumed to be proportional to algal production. Thus, every unit of algal production increases the organic carbon pool by exudates of e_{\max} . A unit of algal net biomass production is completely ingested by the predator and converted either to predator excretion of $(1 - \varepsilon)$, respiration r_R or production P_A . Additionally to algal exudation, predator excretion supplies the carbon pool, which is consumed by bacteria. The bacteria respire parts of this carbon while they invest the rest into biomass production, which is completely taken up by the predator at steady state. Parts of this ingested bacterial production returns to the carbon pool by excretion. We resolve this loop by a geometric series. After respiratory losses, this results in a predator production from

bacteria (P_B) which originated from one unit of algal production. The predator production per unit algal production from algae (P_A) and bacteria (P_B) thus becomes

$$\begin{aligned} P_A &= \varepsilon (1 - r_R) \\ P_B &= (e_{\max} + (1 - \varepsilon)) \frac{1}{1 - (1 - r_B)(1 - \varepsilon)} (1 - r_B) \varepsilon (1 - r_R) \end{aligned} \quad (1)$$

From Eq. 1, we can compute the fraction of predator production that originates from bacteria $P_B/(P_A + P_B)$ and the ratio of predator production with and without bacteria $(P_A + P_B)/P_A$, which gives the increase of predator production caused by the consumption of bacteria additionally to phytoplankton. Notably, these quantities become independent of predator respiration as it cancels out. This reduces the number of influential parameters to the physiological parameters that characterize the favoring and suppressing conditions, which makes these estimates of predator production even more robust and applicable to many species. However, this static model conveys no feed-back on the prey and thus no information on actual

biomasses or population dynamics. Thus, we consider below a mechanistic differential equation model (Eq. 2) to obtain a full picture of the effects of bacteria on phytoplankton–zooplankton interactions.

Dynamic phytoplankton–zooplankton model with organic carbon pool and bacteria

Using a well-established model presented by Fussmann et al. (2000) and Yoshida et al. (2003), we describe the predator–prey interaction of the rotifer *Brachionus calyciflorus* (R, Ind./L) feeding on its natural prey, the unicellular green algae *Monoraphidium minutum* (A, cells/L) in a chemostat (Fig. 1b). We simplify the original model slightly by assuming that every rotifer individual is fertile, i.e., we neglect the short periods of juvenile growth and senescence, but extend it by adding a pool of organic carbon C ($\mu\text{mol L}^{-1}$) and bacteria B (cells/L). Nitrogen N ($\mu\text{mol L}^{-1}$) is the limiting resource for algal growth. Bacterial growth is assumed to be multiplicatively co-limited by nitrogen and carbon. The full model reads.

$$\begin{aligned} \frac{dN}{dt} &= \delta N_i + (1 - \varepsilon) \omega_{R,N} (F_{R,A} + F_{R,B}) R - \omega_{A,N} F_A A - \omega_{B,N} F_B B - \delta N \\ \frac{dC}{dt} &= \frac{e_{\text{dyn}}}{1 - e_{\text{min}}} \omega_{A,C} \beta_A A + (1 - \varepsilon) \omega_{R,C} (F_{R,A} + F_{R,B}) R - \frac{1}{1 - r_B} \omega_{B,C} F_B B - \delta C \\ \frac{dA}{dt} &= F_A A - \frac{\omega_{R,C}}{\omega_{A,C}} F_{R,A} R - \delta A \\ \frac{dB}{dt} &= F_B B - \frac{\omega_{R,C}}{\omega_{B,C}} F_{R,B} R - \delta B \\ \frac{dR}{dt} &= (1 - r_R) \varepsilon (F_{R,A} + F_{R,B}) R - \delta R \end{aligned} \quad (2)$$

All parameter values are listed in Table 1 along with their biological meaning (for a detailed discussion see Supporting Information Appendix 1). We will now describe the terms of the model in the order as they appear in Eq. 2.

The nitrogen pool in the chemostat is supplied by the inflow of fresh medium, which is given by the product of chemostat dilution rate δ and nitrogen concentration in the medium N_i , and the excretion of the predators from feeding on algae and bacteria. Algal and bacterial growth, at per capita rates F_i (Eq. 3), and wash-out reduce the nitrogen pool.

Exudation by algae is assumed to be proportional to algal carbon fixation, whereas the proportionality factor increases linearly toward a maximum as the algal nutrient limitation increases (e_{dyn} , see Supporting Information Appendix 2 and Supporting Information Fig. S1). This dynamic, nutrient dependent exudation by algae, together with the excretion by predators maintains the carbon pool. Carbon is diminished by bacterial consumption and wash-out. The interactions of species i with the carbon and nutrient pools are scaled by the respective carbon ($\omega_{i,C}$) and nitrogen ($\omega_{i,N}$) content of an individual.

Algae and bacteria grow at per capita growth rates [d^{-1}] of

$$\begin{aligned} F_A &= \beta_A \frac{1 - e_{\text{dyn}}}{1 - e_{\text{min}}} \frac{N}{H_A + N} \\ F_B &= \beta_B \frac{C}{H_{B,C} + C} \frac{N}{H_{B,N} + N} \end{aligned} \quad (3)$$

where β_i is the maximum growth rate of species i , e_{min} is the minimum exudation and H_i is the half saturation constant. Algal and bacterial densities are reduced by predator grazing and wash-out. The predator per capita grazing rates on algae and bacteria [d^{-1}] follow a multi-species Holling Type-II shape (Eq. 4).

$$\begin{aligned} F_{R,A} &= G \frac{\omega_{A,C} A}{H_R + \omega_{A,C} A + p_B \omega_{B,C} B} \\ F_{R,B} &= G \frac{p_B \omega_{B,C} B}{H_R + \omega_{A,C} A + p_B \omega_{B,C} B} \end{aligned} \quad (4)$$

Here, G is the maximum grazing rate of a predator and H_R is the half saturation constant scaled to carbon. The bacteria are potentially less edible than the algae, depending on the degree of bacterivory of the predators p_B which provides the part of the bacterial population that is accessible to the predator. Effectively, this scales up the half-saturation constant of the predator for feeding on bacteria. Grazing is converted into bacterial or algal losses by the ratio of carbon contents per individual. The predators assimilate only a part of the ingested food. What is not assimilated is excreted and enters the carbon pool. The assimilates are further reduced by respiration, the remainders are used for production of new predator biomass. The only loss-term of predators is wash-out.

Numerical simulations and determination of dynamics

To achieve a broad picture of the effects of bacteria, we examined the parameter space spanned by the dilution rate of the chemostat δ and the degree of bacterivory of the predator p_B , thereby considering the two scenarios suppressing or favoring bacteria. The dilution rate is an important parameter for the performance of the individual species as it determines the rate of nutrient input and the loss rates of all species. The degree of bacterivory is important as it shapes the interspecific interactions via the apparent competition between algae and bacteria mediated by the predator. A third important system parameter is the nutrient inflow concentration N_i , which we included in our analysis at an intermediate dilution rate for favoring conditions.

The system of ordinary differential equations Eq. 2 was integrated with the *odeint* package from the Scipy library (Jones et al. 2001) in Python (version 3.5).

The presence of bacteria in an algae–rotifer system may have two ecologically important effects, first on the mean biomasses, which can directly be obtained from the model

outputs, and second on the population dynamics. To distinguish between steady state, regular cycles, and irregular dynamics, local peaks in the normalized autocorrelation function (nACF) of the algal density were detected using the *argrelmax* algorithm from Scipy. A time series was classified as being at steady state if no peaks with prominence above the accuracy of the solver were detected. If the first peak of the nACF was above 0.95 the dynamics are periodic and were classified as regular. We termed the population dynamics of one such period the *repetitive unit* and extracted the number of algal maxima from it. If all peaks of the nACF were below 0.95 the dynamics show no clear repetitive pattern and thus were classified as irregular.

Assessment

Effect of bacteria on predator production

The static carbon flux model predicts a dependence of predator production on maximal algal exudation e_{\max} , predator assimilation efficiency ϵ and bacterial respiration r_B (Fig. 2). The model justifies the rationale behind the maximum and minimum impact scenarios, i.e., bacteria-favoring and -suppressing conditions, respectively. Predator production is least strongly affected by the presence of bacteria at low algal exudation, low predator excretion and low bacteria growth efficiency. The model predicts that under these bacteria-suppressing conditions 14% of the total predator production originate from ingesting bacteria. This results in an increase of total predator production by 16%. In contrast, under bacteria-favoring conditions bacteria constitute 48% of total predator production, which almost doubles with an increase by 94%. From this simplified model, we already see that bacteria may have a large effect under certain physiological conditions.

Effect of bacteria on mean biomasses

Using the mechanistic model, we compare the effect of bacteria in chemostat experiments under suppressing and favoring conditions for large ranges of the chemostat dilution rate δ and the degree of bacterivory of the predator p_B . These two key parameters, which govern the fluxes in the system, may strongly affect the mean biomasses of all species (Fig. 3). Comparing the two extreme cases of bacteria-suppressing vs. bacteria-favoring conditions shows that under suppressing conditions bacterial biomass remains mostly negligible and algal and predator biomass is thus independent of the degree of bacterivory by the predator (Fig. 3a). With little bacteria present algal mean biomass increases and predator biomass decreases as the dilution rate increases. Only at very low degrees of bacterivory and high dilution rates the bacteria can achieve non-negligible biomasses, which is reflected by a slightly lower algal biomass in this parameter region.

In contrast, under bacteria-favoring conditions bacteria reach considerable mean biomasses, which are highest at low degrees of bacterivory and high dilution rates (Fig. 3b). An increasing degree of bacterivory results in lower bacterial and higher predator biomass. The algal biomass increases due to a release from competition. At very strong bacterivory and low dilution rate bacterial mean biomass becomes negligible in favor of the algae. The predator goes extinct if the dilution rate exceeds its maximal realized per capita growth rate. The dilution rates that the predator can withstand increase with stronger bacterivory.

The effect size of bacteria represented by the logarithmic ratio of mean biomasses in simulations with and without bacteria provides a direct measure of the impact of bacteria on mean biomasses (Fig. 4, Supporting Information Fig. S2). While for suppressing conditions the bacterial biomass and thus the effect size of bacteria is negligible throughout the parameter space (Supporting Information Fig. S2), interesting

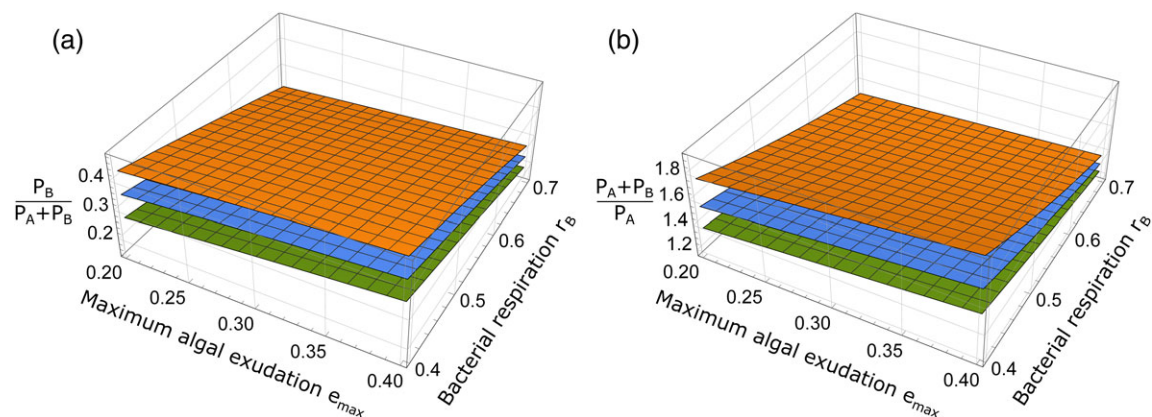


Fig. 2. Impact of bacteria on predator production as predicted by the static model. Depending on the exudation, i.e., the fraction of carbon that is maximally exudated by algae e_{\max} , the bacterial respiration, i.e., the fraction of carbon taken up by bacteria that is respired r_B , and the assimilation efficiency of predators ϵ , bacteria can contribute a significant portion to predator production. The assimilation efficiency is set to 0.4 (orange, top), 0.55 (blue, middle), and 0.7 (green, bottom). **(a)** Predator production derived from bacteria (P_B) relative to total predator production ($P_A + P_B$). **(b)** Total predator production with bacteria present relative to the predator production without bacteria.

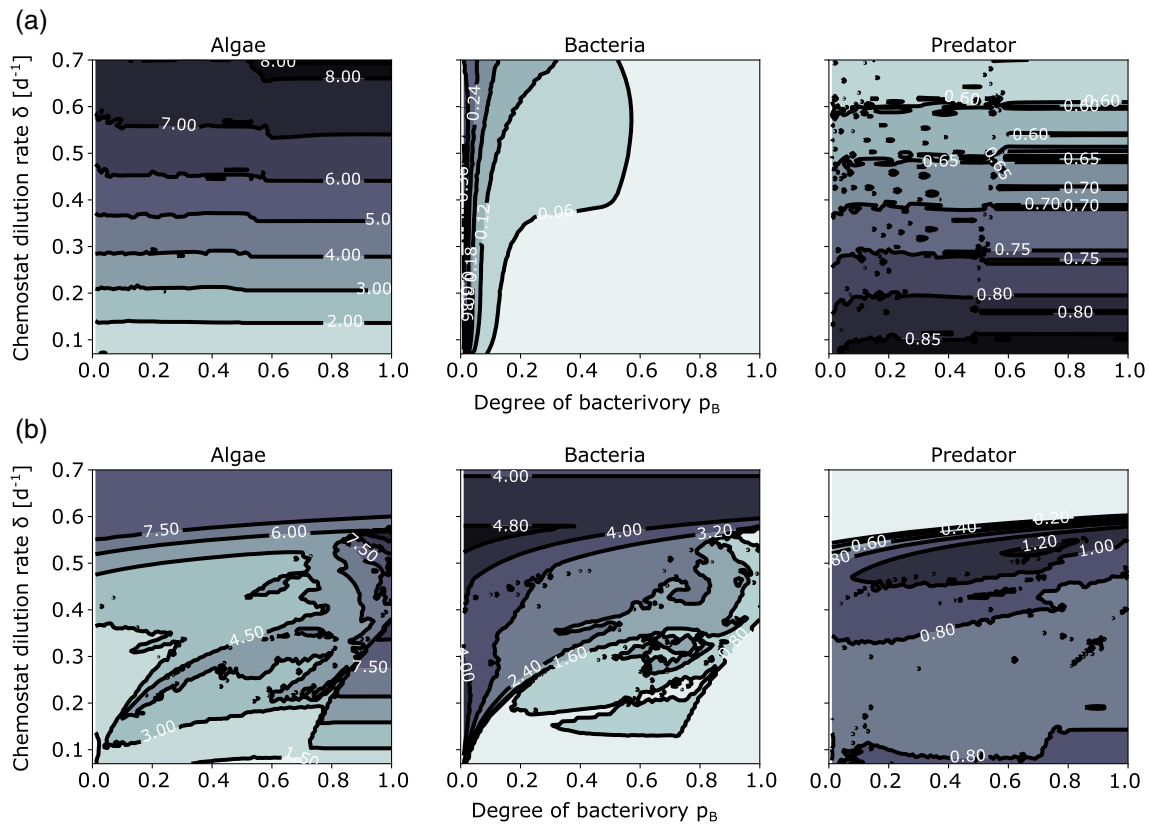


Fig. 3. Mean biomasses for (a) suppressing conditions (algal exudation, predator excretion, and bacterial growth efficiency are low) and (b) favoring conditions for bacteria (algal exudation, predator excretion, and bacterial growth efficiency are high) for the parameter space spanned by the chemostat dilution rate δ and the degree of bacterivory of the predator p_B . Colors correspond to different biomass levels [mgC/L] in the individual plots as the biomass ranges vary largely.

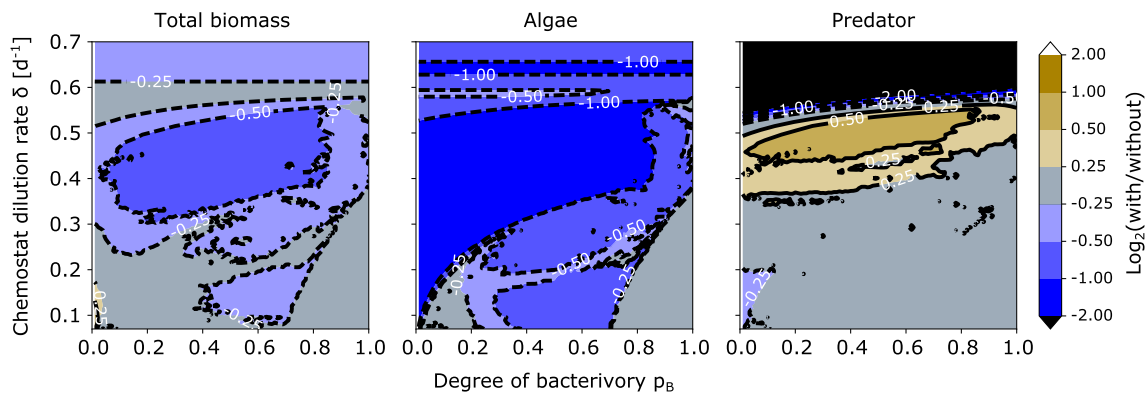


Fig. 4. Effect size of bacterial presence under bacteria-favoring conditions. The effect size is defined as the logarithmic ratio to base 2 of the mean biomasses with and without bacteria. The presence of bacteria often decreases algal and total biomass but mostly increases predator biomass. Under suppressing conditions, the bacteria have only little effect (see Supporting Information Fig. S2).

patterns emerge for favoring conditions (Fig. 4). Here, the total biomass in the chemostat, i.e., the sum of algae, predators, and bacteria in units of carbon per liter decreases strongly if bacterivory and dilution rates are at intermediate levels, which originates from low algal biomasses that are not compensated by the bacteria and the biomass increase of the predator.

Effect of bacteria on population dynamics

Population dynamics are often used as fingerprints of biological interactions. To study how they are affected by the presence of bacteria, we evaluated the type of population dynamics in the parameter space of Figs. 3, 4 for the bacteria-favoring scenario where bacteria have a significant effect on

the mean biomasses (Figs. 5, 6). We found a complex pattern of alternating regions of regular and non-regular dynamics (Fig. 5).

At low dilution rates and high to intermediate degrees of bacterivory, the population dynamics are fairly simple (panels i and ii in Fig. 6). Within a cycle the algae establish first, nitrogen declines and organic carbon accumulates which allows the bacteria to increase as well. Finally, the predator reaches high biomasses by grazing down both algae and bacteria. This releases the nitrogen, the predator declines and the whole cycle starts again. However, if the degree of bacterivory is too high, the bacteria go extinct (as in panel i). These classic predator-prey cycles can easily become highly complex, driven by the interaction of direct and indirect competition between algae and bacteria (panels iii, iv, and v). For a fairly low degree of bacterivory and a low dilution rate, the predators increase for a second time within one cycle of the overall population dynamics (termed *repetitive unit*) even though algal densities are already too low to enable predator net growth (panel iii). This second predator peak is mainly realized from grazing on bacteria and shows that the presence of bacteria can strongly alter the shape of the predator population dynamics.

For broad parameter ranges multiple algal maxima occur within one repetitive unit (panel iv) and partly the dynamics become irregular, i.e., no repetitive unit can be found in the time-series of the biomasses (panel v). Here, algae and bacteria alternate during the increase of the predator. Bacteria are the better competitors for nitrogen, but rely on the carbon exudates from the algae. Thus, the algal biomass increases first, but is soon reduced mainly by washout since predation pressure is still very low due to the low predator biomass. Algae

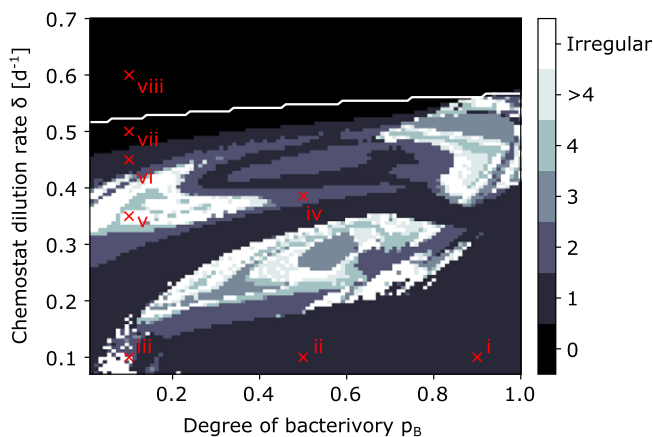


Fig. 5. Population dynamics under favoring conditions determined by the number of algal peaks within a repetitive unit, i.e., the shortest periodic element. If no such unit was found the dynamics are classified as irregular, or steady state if no oscillations occurred at all. Mean predator biomass drops below 10^{-30} mgC/L above the white line. The dynamics can become highly complex, unless bacteria are grazed down by the predator, which happens for high degrees of bacterivory p_B and low chemostat dilution rates δ .

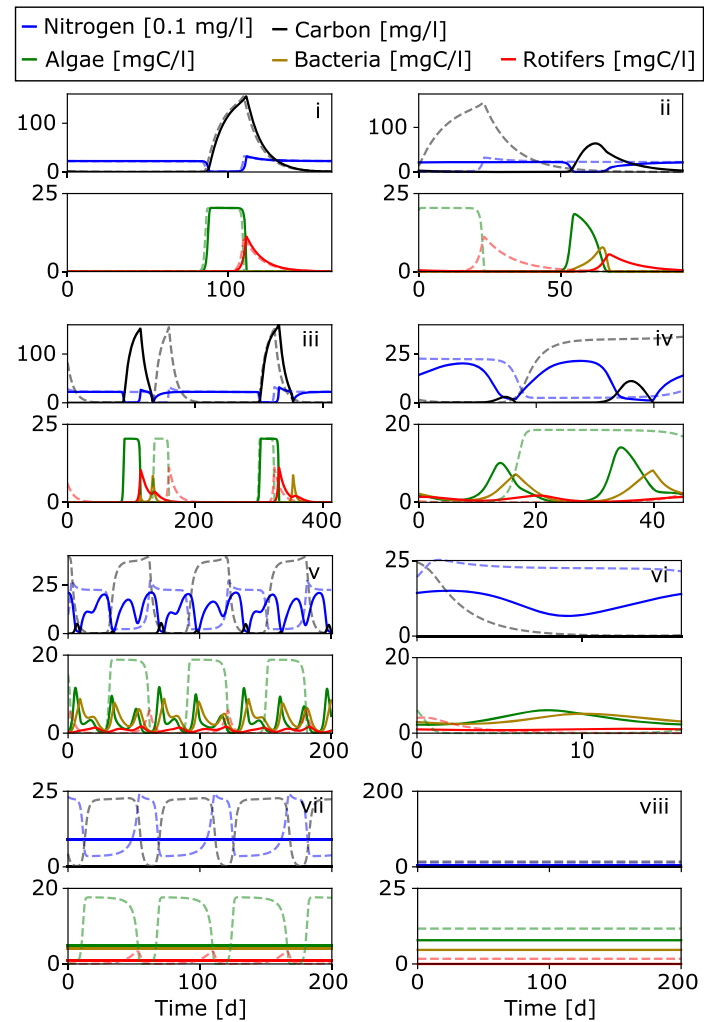


Fig. 6. Time series for the marked parameter combinations in Fig. 5. Solid and dashed lines correspond to simulation runs with and without bacteria present, respectively. The drastic differences between the simulations with and without bacteria show that bacteria can strongly affect the population dynamics. The dynamics were characterized from the dynamics with bacteria included. If a periodicity could be determined, the repetitive unit is shown, otherwise the dynamics are plotted for 200 d. Periodic dynamics contain either one (panels i, ii, vi) or multiple prey maxima within a repetitive unit (panels iii and iv). Steady states are shown in panels vii, where all species coexist, and viii, where the predator went extinct. Non-periodic dynamics were termed irregular and are shown in panel v. In panel iii, the predator reaches a first maximum from grazing down algae and bacteria. This results in excretions from which the bacteria increase a second time, allowing also the predator to increase again. It is only possible to explain this second predator peak by also considering bacteria.

are washed out at higher nitrogen concentrations than bacteria given their higher half-saturation constants. The bacteria, however, are washed out when the carbon is depleted. This increases the nitrogen concentration and allows the algae to increase again. Eventually, the predator has accumulated enough biomass to graze down both algae and bacteria. Without further food, the predator is now washed out and the

whole cycle starts again. At high dilution rates the cycle amplitude decreases (panel vi) and eventually the dynamics reach a steady state (panel vii). If the predator goes extinct, algae and bacteria continue to coexist in a steady state (panel viii).

Explanation of results

The combined effect of dilution rate and degree of bacterivory can be understood by shifts in the balance between bottom-up and top-down control (Figs. 5, 6). At high dilution rates and low degrees of bacterivory the predator is strongly limited in its net growth and the prey becomes more bottom-up limited (Fig. 6, panels vi, vii, and viii). Thus, its cycle amplitudes decrease and mean biomasses increase. The low top-down control allows the prey to first deplete the resources before being washed out, in parts of the parameter space for multiple times during one predator cycle, before the predator has caught up and finally grazes down the prey (Fig. 6, panels iv and v). Within this first phase of low top-down control competition between algae and bacteria alternates with algae supporting bacterial growth through the release of organic carbon, which explains the complex multi-cycle patterns. At low dilution rates and high degrees of bacterivory, the top-down control increases as the predator is able to exert a considerable predation pressure on both algae and bacteria, thus forcing the system into more regular predator-prey cycles (Fig. 6, panels i and ii). The second predator peak (Fig. 6, panel iii) arises if the predation pressure is strong enough to quickly reduce algal biomass, while exudates are not yet washed out. This remaining carbon, together with the low degree of bacterivory, creates a short window of opportunity of high bacterial biomass, which then results in a peak in the predator's biomass without high algal biomasses.

Effect of nutrient inflow concentration

Similar to the above results, also the parameter space spanned by nutrient inflow concentration and degree of bacterivory is composed of regions of different bottom-up-top-down balances. As the inflow concentration increases the chemostat system is enriched and all mean biomasses increase (Supporting Information Fig. S3a). An increasing degree of bacterivory has a similar effect for the predator as it broadens its food spectrum. Also, higher degrees of bacterivory suppress bacteria and favor algae in their apparent competition. Thus, if both parameters are low there is strong bottom-up control and the effect size of bacteria on the total biomass and the algae is small (Supporting Information Fig. S3b). If nutrient inflow concentration and degree of bacterivory are high this results in a strong top-down control which again decreases the effect size of bacteria on the total biomass and the algae. In intermediate parameter ranges, however, both total biomass and algae are strongly negatively affected by bacteria. The effect size of bacteria on the predator behaves contrary. In the parameter regions of high bottom-up control and high top-

down control, the predator is affected negatively, whereas it largely benefits from the bacteria in the intermediate region.

The dynamic pattern approximately reflects these three regions with simpler dynamics at strong forcing and more complex dynamics in the intermediate regime (Supporting Information Fig. S3c).

Discussion

Chemostat experiments, particularly with phytoplankton-zooplankton systems, are often employed to resolve ecological and evolutionary questions regarding predator-prey interactions. However, bacteria are omnipresent actors in nature. In this paper, we argue that it may be indispensable to either include bacteria in the interpretation of study results or to take applicable measures to minimize their effect.

Using a simplified, static carbon-flux model as well as a mechanistic, dynamic chemostat model, which has been parametrized closely to typical experimental systems, we show that bacteria are able to strongly impact predator production, biomass levels and population dynamics in chemostat experiments. Under bacteria-suppressing conditions, i.e., if specific physiological properties of the organisms reduce the production and utilization of organic carbon, we expect bacteria to generally play only a minor role, if at all. Under bacteria-favoring conditions, however, predator production is substantially increased by the presence of bacteria. It is important to note that the contribution of bacteria to predator ingestion varies in time and thus temporally exceeds the mean values predicted by the static carbon-flux model. From the dynamic model, we see that the effect of bacteria on the biomasses and particularly the population dynamics in the chemostat strongly depends on the experimental conditions, i.e., the dilution rate and nutrient inflow concentration, as well as the degree of bacterivory of the predators.

Impact of the bacterial pathway on the food web structure

The shift of biomass from algae to bacteria at intermediate dilution rates and bacterivory decreases the total biomass in the chemostat when comparing systems with and without bacteria present. Here, the biomass of the bacteria and the biomass increase of the predator are not sufficient to compensate for the biomass losses of the algae as the bacterial pathway in the food web includes bacterial respiration as an additional loss-term along which biomass is irretrievably lost. This may obstruct predictions for biomass yield and energy balances in aquatic mass cultures if bacteria were not considered (Hino et al. 1997). On the other hand, this pathway increases the predator biomass as now algal exudates and predator excretion, which are lost without bacteria, are recycled by the bacteria and may be used by the predator, thus increasing the efficiency by which primary production is transferred to the predator.

Importance of bacteria for population dynamics

While for high degrees of bacterivory and low dilution rates we observed regular predator–prey cycles, the dynamics can become highly complex for intermediate parameter regions. Within one pronounced and experimentally detectable cycle of the predator multiple cycles of algae and bacteria can occur. At low bacterivory and low dilution rates, the overall dynamics resemble those without bacteria at first glance. The only indication of bacteria having an effect in this region is the second predator peak, which cannot be explained without considering bacteria in an experimental chemostat system and instead might lead to wrong conclusions.

A recent model study showed that already small changes in food web structure, such as introducing a second predator with a slightly different prey preference, may result in intermittent cycles (Bengfort et al. 2017). We showed that including bacteria in a chemostat model may cause similar deviations from the expected predator–prey interactions. Population dynamics observed in chemostat experiments are occasionally quite irregular (G. Weithoff pers. comm.; Bengfort et al. 2017) and it remains to be studied whether this irregularity is just a more complex attractor similar to the ones observed in this study. Bacteria could thus be an overlooked actor in chemostat experiments responsible for unexpected complexity of population dynamics.

Impact of bacteria when inferring processes from patterns

A prominent example of eco-evolutionary feedbacks is the evolution of defense in prey populations under predation, resulting in a temporal niche for a defended, less palatable clone when the predation pressure is high (Becks et al. 2012). As long as the defended prey dominates predator biomass decreases and a niche opens for the undefended prey if it is more competitive for nutrients than the defended prey. These interactions result in dynamics similar to those presented in Fig. 6, panels ii and iv. Here, the algae increase first and their exudation provides a temporal niche for bacteria. Thus, bacteria depend on the algae, even though algae and bacteria also compete for nitrogen. Recently, we showed that a similar combination of facilitation and competition between two prey species can ensure their coexistence (Raatz et al. 2017). Such sustained coexistence by temporal niching results in a prolonged total prey biomass peak (here the sum of algae and bacteria) and a delayed predator response, which both are characteristic for eco-evolutionary dynamics (Yoshida et al. 2003; van Velzen and Gaedke 2017). Thus, by merely inferring a process from a pattern without acknowledging the presence of bacteria may overestimate the importance of eco-evolutionary dynamics.

Implications for improvement of experimental design

Our study enables us to propose means for reducing the impact of bacteria in chemostat studies that explicitly focus on phytoplankton–zooplankton interactions by adjusting

their design accordingly. Aside from the easily implemented measure to reduce the dilution rate, which enables a stronger response by the predator, also the ability to ingest bacteria should be taken into account when the predator species is selected. Instead of intuitively using species incapable of ingesting bacteria (e.g., numerous *rotifers*, Arndt 1993), predator species with a high degree of bacterivory could be the preferred choice (e.g., many *ciliates*, Sherr and Sherr 1987).

Bacteria can affect phytoplankton–zooplankton interactions in a chemostat by two mechanisms: (1) by competing for nutrients with the algae and (2) by contributing to predator production. When we considered the effect sizes as a measure of the ratio of average biomasses with and without bacteria the zero-bacterivory limit corresponds to the case when only competition is at play. A high degree of bacterivory, however, includes the effect of both competition and predator divergence. Since the effect sizes do not vanish toward low degrees of bacterivory we see that bacteria have a considerable competitive impact on the algae and thus affect the food web even if they do not contribute to the production of the predator. A high degree of bacterivory of the predator minimizes the competitive impact of bacteria and thus decreases the effect of bacteria in chemostat experiments.

Here, we argue that bacteria are an unavoidable and inherent actor in phytoplankton–zooplankton chemostats, whose impact may be minimized by choosing the right experimental setup. Thereby, we should keep in mind that—up to now overlooked—bacteria might have some impacts on population dynamics and species coexistence that are comparable to the previously overlooked effects of rapid evolution (Yoshida et al. 2003).

Our study shows that only with an appropriate choice of the predator species and an appreciation for the presence and role of all important actors, we can correctly interpret phytoplankton–zooplankton chemostats and use them to study complex predator–prey interactions.

References

- Anderson, T. R., and H. W. Ducklow. 2001. Microbial loop carbon cycling in ocean environments studied using a simple steady state model. *Aquat. Microb. Ecol.* **26**: 37–49. doi:[10.3354/ame026037](https://doi.org/10.3354/ame026037)
- Aoki, S., and A. Hino. 1996. Nitrogen flow in a chemostat culture of the rotifer *Brachionus plicatilis*. *Fish. Sci.* **62**: 8–14. doi:[10.2331/fishsci.62.8](https://doi.org/10.2331/fishsci.62.8)
- Arndt, H. 1993. Rotifers as predators on components of the microbial web (bacteria, heterotrophic flagellates, ciliates)—a review. *Hydrobiologia* **255–256**: 231–246. doi:[10.1007/BF00025844](https://doi.org/10.1007/BF00025844)
- Baines, S. B., and M. L. Pace. 1991. The production of dissolved organic matter by phytoplankton and its importance to bacteria: Patterns across marine and freshwater systems.

- Limnol. Oceanogr. **36**: 1078–1090. doi:10.4319/lo.1991.36.6.1078
- Becks, L., S. P. Ellner, L. E. Jones, and N. G. Hairston Jr. 2010. Reduction of adaptive genetic diversity radically alters eco-evolutionary community dynamics. *Ecol. Lett.* **13**: 989–997. doi:10.1111/j.1461-0248.2010.01490.x
- Becks, L., S. P. Ellner, L. E. Jones, and N. G. Hairston. 2012. The functional genomics of an eco-evolutionary feedback loop: Linking gene expression, trait evolution, and community dynamics. *Ecol. Lett.* **15**: 492–501. doi:10.1111/j.1461-0248.2012.01763.x
- Bengfort, M., E. van Velzen, and U. Gaedke. 2017. Slight phenotypic variation in predators and prey causes complex predator-prey oscillations. *Ecol. Complex.* **31**: 115–124. doi:10.1016/j.ecocom.2017.06.003
- Bratbak, G., and T. Thingstad. 1985. Phytoplankton-bacteria interactions: An apparent paradox? Analysis of a model system with both competition and commensalism. *Mar. Ecol. Prog. Ser.* **25**: 23–30. doi:10.3354/meps025023
- Declerck, S. A. J., A. R. Malo, S. Diehl, D. Waasdorp, K. D. Lemmen, K. Proios, and S. Papakostas. 2015. Rapid adaptation of herbivore consumers to nutrient limitation: Eco-evolutionary feedbacks to population demography and resource control. *Ecol. Lett.* **18**: 553–562. doi:10.1111/ele.12436
- del Giorgio, P. A., and J. J. Cole. 1998. Bacterial growth efficiency in natural aquatic systems. *Annu. Rev. Ecol. Syst.* **29**: 503–541. doi:10.1146/annurev.ecolsys.29.1.503
- Dumont, H. J., I. Van de Velde, and S. Dumont. 1975. The dry weight estimate of biomass in a selection of Cladocera, Copepoda and Rotifera from the plankton, periphyton and benthos of continental waters. *Oecologia* **19**: 75–97. doi:10.1007/BF00377592
- Fussmann, G. F., S. P. Ellner, K. W. Shertzer, and N. G. J. Hairston. 2000. Crossing the hopf bifurcation in a live predator-prey system. *Science* **290**: 1358–1360. doi:10.1126/science.290.5495.1358
- Gaedke, U., S. Hochstädter, and D. Straile. 2002. Interplay between energy limitation and nutritional deficiency: Empirical data and food web models. *Ecol. Monogr.* **72**: 251–270. doi:10.1890/0012-9615(2002)072[0251:IBELAN]2.0.CO;2
- Hiltunen, T., L. E. Jones, S. P. Ellner, and N. G. Hairston. 2013. Temporal dynamics of a simple community with intraguild predation: An experimental test. *Ecology* **94**: 773–779. doi:10.1890/12-0786.1
- Hino, A., S. Aoki, and M. Ushiro. 1997. Nitrogen-flow in the rotifer *Brachionus rotundiformis* and its significance in mass cultures. *Hydrobiologia* **358**: 77–82. doi:10.1023/A:1003128305910
- Humphreys, W. F. 1979. Production and respiration in animal populations. *J. Anim. Ecol.* **48**: 427–453. doi:10.2307/4171
- Ishino, R., S. Iehata, M. Nakano, R. Tanaka, T. Yoshimatsu, and H. Maeda. 2012. Bacterial diversity associated with the rotifer *Brachionus plicatilis* sp. complex determined by culture-dependent and -independent methods. *Biocontrol Sci.* **17**: 51–56. doi:10.4265/bio.17.51
- Jensen, T. C., T. R. Anderson, M. Daufresne, and D. O. Hessen. 2006. Does excess carbon affect respiration of the rotifer *Brachionus calyciflorus* Pallas? *Freshw. Biol.* **51**: 2320–2333. doi:10.1111/j.1365-2427.2006.01653.x
- Jones, E., T. Oliphant, and P. Peterson 2001 SciPy: Open source scientific tools for Python.
- Morris, D. P., and W. M. Lewis. 1992. Nutrient limitation of bacterioplankton growth in Lake Dillon, Colorado. *Limnol. Oceanogr.* **37**: 1179–1192. doi:10.4319/lo.1992.37.6.1179
- Novick, A., and L. Szilard. 1950. Description of the chemostat. *Science* **112**: 715–716. doi:10.1126/science.112.2920.715
- Ooms-Wilms, A. L. 1997. Are bacteria an important food source for rotifers in eutrophic lakes? *J. Plankton Res.* **19**: 1125–1141. doi:10.1093/plankt/19.8.1125
- Raatz, M., U. Gaedke, and A. Wacker. 2017. High food quality of prey lowers its risk of extinction. *Oikos* **126**: 1501–1510. doi:10.1111/oik.03863
- Rothhaupt, K. O. 1990. Differences in particle size-dependent feeding efficiencies of closely related rotifer species. *Limnol. Oceanogr.* **35**: 16–23. doi:10.4319/lo.1990.35.1.0016
- Seah, B. K. B., T. Schwaha, J.-M. Volland, B. Huettel, N. Dubilier, and H. R. Gruber-Vodicka. 2017. Specificity in diversity: Single origin of a widespread ciliate-bacteria symbiosis. *Proc. R. Soc. London B Biol. Sci.* **284**: 20170764. doi:10.1098/rspb.2017.0764
- Sherr, E. B., and B. F. Sherr. 1987. High rates of consumption of bacteria by pelagic ciliates. *Nature* **325**: 710–711. doi:10.1038/325710a0
- Starkweather, P. L., J. J. Gilbert, and T. M. Frost. 1979. Bacterial feeding by the rotifer *Brachionus calyciflorus*: Clearance and ingestion rates, behavior and population dynamics. *Oecologia* **44**: 26–30. doi:10.1007/BF00346392
- Straile, D. 1997. Gross growth efficiencies of protozoan and metazoan zooplankton and their dependence on food concentration, predator-prey weight ratio, and taxonomic group. *Limnol. Oceanogr.* **42**: 1375–1385. doi:10.4319/lo.1997.42.6.1375
- Tittel, J., O. Büttner, and N. Kamjunke. 2012. Non-cooperative behaviour of bacteria prevents efficient phosphorus utilization of planktonic communities. *J. Plankton Res.* **34**: 102–112. doi:10.1093/plankt/fbr094
- Vadstein, O., L. M. Olsen, A. Busch, T. Andersen, and H. R. Reinertsen. 2003. Is phosphorus limitation of planktonic heterotrophic bacteria and accumulation of degradable DOC a normal phenomenon in phosphorus-limited systems? A microcosm study. *FEMS Microbiol. Ecol.* **46**: 307–316. doi:10.1016/S0168-6496(03)00195-8
- van Velzen, E., and U. Gaedke. 2017. Disentangling eco-evolutionary dynamics of predator-prey coevolution: The

case of antiphase cycles. *Sci. Rep.* **7**: 1–11. doi:[10.1038/s41598-017-17019-4](https://doi.org/10.1038/s41598-017-17019-4)

Vrede, K., M. Heldal, S. Norland, and G. Bratbak. 2002. Elemental composition (C, N, P) and cell volume of exponentially growing and nutrient-limited bacterioplankton. *Appl. Environ. Microbiol.* **68**: 2965–2971. doi:[10.1128/AEM.68.6.2965-2971.2002](https://doi.org/10.1128/AEM.68.6.2965-2971.2002)

Yoshida, T., L. E. Jones, S. P. Ellner, G. F. Fussmann, and N. G. Hairston. 2003. Rapid evolution drives ecological dynamics in a predator-prey system. *Nature* **424**: 303–306. doi:[10.1038/nature01767](https://doi.org/10.1038/nature01767)

Acknowledgments

This work was funded by DFG (WA 2445/8-2, WA 2445/11-1, GA 401/26-1) as part of the Priority Programme 1704 (DynaTrait).

Conflict of Interest

None declared.

Submitted 26 April 2018

Accepted 09 July 2018

Associate editor: Gordon Holtgrieve

One man's trash is another man's treasure - the effect of bacteria on phytoplankton-zooplankton interactions in chemostat systems

Supporting Information

M Raatz^{*1}, S Schällicke¹, M Sieber², A Wacker¹, and U Gaedke¹

¹University of Potsdam, Institute of Biochemistry and Biology, Department of Ecology and Ecosystem Modelling, Potsdam, Germany

²Max-Planck Institute for Evolutionary Biology, Department Evolutionary Theory, Plön, Germany

DOI: 10.1002/lom3.10269

Appendix 1 - Parameter choice

Parameters for the maximum and minimum impact scenarios

Reports on algal exudation are highly variable. A meta-analysis found that the ratio of exudates relative to primary production varies between 2.82% and 42.1%, whereas 10 out of 16 systems that were included in the analysis had values above 10% (Baines and Pace 1991). Thus, we set the minimum exudation to $e_{\min} = 0.1$. For bacteria-suppressing conditions we set a maximum exudation of $e_{\max} = 0.2$, under favoring conditions, we assumed $e_{\max} = 0.4$. In another meta-analysis bacterial growth efficiencies on carbon that was excreted by phytoplankton were found to range from 0.3 to 0.8 (del Giorgio and Cole 1998). This corresponds to values for the respiration parameter r_B between 0.2 and 0.7. Accordingly, we set the bacterial respiration to $r_B = 0.7$ for the bacteria-suppressing conditions, but remain conservative and only set $r_B = 0.4$ for the bacteria-favoring scenario, as the carbon pool in our study also consists of rotifer excretion which is typically not as easily processible as algal exudates. Rotifer gross growth efficiency was found to range from 0.1 to 0.4 (Straile 1997). This also includes rotifer respiration r_R , which we set to 0.5 (Humphreys 1979), and therefore corresponds to carbon assimilation efficiencies between 0.2 and 0.8. Again, we remain conservative and choose $\varepsilon = 0.4$ for bacteria-suppressing conditions and $\varepsilon = 0.7$ for bacteria-favoring conditions.

Chemostat parameters

In an experiment, the parameters for dilution rate and resource nitrogen concentration in the inflow medium have to be set according to the needs of the species under study. The setting for the dilution rates should be reasonable in comparison to the typical prey and predator growth rates, so that both are able to achieve substantial positive net growth. For fast growing prey, such as *Chlorella* in Fussmann et al. (2000), higher dilution rates are possible, but also examples of very low dilution rates exist and are equally valid (Vadstein et al. 2003). The same reasoning applies to the inflow concentration where also different values are regularly used and adjusted to the species and research goals (Becks et al. 2010; Fussmann et al. 2000). Hence, we cover a large range of δ and N_I in our analysis.

Algae parameters

Generally, algal morphology is diverse and results in broad possible parameter ranges. We chose to parametrize the algae according to *Monoraphidium minutum*, which is used as food to sustain our lab cultures of *Brachionus calyciflorus* and has also been used by others as prey in experiments with

*michael.raatz@uni-potsdam.de

zooplankton (Rothhaupt 1992; Rothhaupt 1990b). It is generally similar to other small green algae like *Chlorella* or *Chlamydomonas*, which are also commonly used in chemostat experiments (Becks et al. 2010; Yoshida et al. 2003). Typically, when grown alone in a chemostat with an inflow concentration of $N_I = 80 \mu\text{molN/L}$ and a dilution rate of $\delta = 0.55 \text{d}^{-1}$ *Monoraphidium* will achieve maximum biomass densities around 10mgC/L and cell densities of $1.75 \times 10^9 \text{cells/L}$ (unpublished data, personal communication G. Weithoff, S. Schällicke). This results in an approximate per-cell carbon content of $\omega_{A,C} = 6 \text{pgC}$. Making the simplifying assumption that all free nitrogen in the chemostat is taken up by the algae, this results in a per-cell nitrogen content of $\omega_{A,N} = 4.6 \times 10^{-8} \mu\text{molN}$. Under the same assumption, the algal growth rate and half-saturation constant were estimated from the initial growth phase in a chemostat to $\beta_A = 1.9 \text{d}^{-1}$ and $H_A = 49 \mu\text{molN/L}$ (unpublished data, Svenja Schällicke).

Bacteria parameters

Also bacteria are highly diverse in the traits that determine growth under chemostat conditions. Large size ranges were reported for bacteria from a eutrophic lake (Gaedke et al. 2004). We chose the average on the log-scale of this study, which results in a carbon content per cell of $\omega_{B,C} = 60 \text{fgC}$, which also agrees with marine bacterioplankton grown in batch cultures (Vrede et al. 2002). Here, depending on nutrient limitation, the bacteria contained between $39 \pm 3 \text{fgC}$ per cell under carbon limitation and $92 \pm 5 \text{fgC}$ per cell under nitrogen limitation. In a chemostat that is run under nitrogen-limiting conditions the bacteria are co-limited by carbon and nitrogen. When the bacterial biomass is low and the carbon pool is high, nitrogen limitation will prevail. While the bacteria consume the carbon pool, nitrogen limitation will become dominant. This results in a range for the atomic C:N ratio, which was found to be 3.8 ± 0.1 under carbon limitation and 7.5 ± 1.2 under nitrogen limitation (Vrede et al. 2002). Since we worked with fixed C:N ratios, we chose the average of those two values, which yields a nitrogen content per cell of $\omega_{B,N} = 8.8 \times 10^{-10} \mu\text{molN}$. Bacterial maximum growth rates cover wide ranges (Morris and Lewis 1992). In this study, the authors observed maximum growth rates as high as 1.7d^{-1} during midsummer, but only 0.24d^{-1} during winter. Bacteria are better competitors for phosphorus at low phosphorus concentrations, while *Monoraphidium* achieves higher uptake rates at high phosphorus concentrations (Rothhaupt 1992). Assuming that this coincides with growth rate and holds also for nitrogen, bacteria have a smaller maximum growth rate, but also a lower nitrogen half-saturation constant than *Monoraphidium*. Thus, again we chose the average of the above values and set the bacterial growth rate $\beta_A = 1 \text{d}^{-1}$, which ensures that *Monoraphidium* is able to outcompete the bacteria at high nutrient concentrations. We set the bacterial nitrogen half-saturation constant $H_{B,N}$ to 1/10th of the algae, which yields $H_{B,N} = 4.9 \mu\text{molN/L}$ and makes the bacteria better competitors for nitrogen when it is scarce. The bacterial half-saturation for organic carbon was taken from literature, $H_{B,C} = 0.83 \mu\text{molC/L}$ (Tittel et al. 2012).

Zooplankton parameters

We chose the rotifer *Brachionus calyciflorus* as the model organism in our study as it is a commonly used predator in chemostat experiments (Becks et al. 2012; Declerck et al. 2015; Fussmann et al. 2000; Shertzer and Ellner 2002). In a typical chemostat with $N_I = 80 \mu\text{molN/L}$ and $\delta = 0.55 \text{d}^{-1}$ and population cycles, the predator reaches densities between 60 and 70 Ind/mL (unpublished data, personal communication G. Weithoff). Assuming that during such a peak all available nitrogen in the chemostat is concentrated in the predator, this results in a per-capita nitrogen content $\omega_{R,N} = 1.2 \times 10^{-3} \mu\text{molN/L}$. Using a published C:N ratio for *B. calyciflorus* of 5.6 (Jensen et al. 2006), this results in a per-capita carbon content $\omega_{R,C} = 6.7 \times 10^{-3} \mu\text{molC}$ which corresponds to 80ngC . The dry weights for this species range between 100 and 450 ng (Dumont et al. 1975). This fits with our assumption of 80ngC as typically about half of the dry weight consists of carbon. The maximum ingestion rate was taken from literature as 288ngC/Indd (Rothhaupt 1990a) and was converted to a maximum specific ingestion rate of $G = 3.6 \text{d}^{-1}$ using the per-capita carbon content. In approximate

agreement with Fussmann et al. (2000), who chose a rotifer half-saturation constant $H_R = 15 \mu\text{molN/L}$, we set H_R to $195 \mu\text{molC/L}$, which can be translated to $18 \mu\text{molN/L}$ by using the C:N ratio of the algae in our study.

References

- Baines, S. B. and Pace, M. L. 1991. The production of dissolved organic matter by phytoplankton and its importance to bacteria: Patterns across marine and freshwater systems. *Limnol. Oceanogr.* 36: 1078–1090.
- Becks, L. et al. 2010. Reduction of adaptive genetic diversity radically alters eco-evolutionary community dynamics. *Ecol. Lett.* 13: 989–997.
- Becks, L. et al. 2012. The functional genomics of an eco-evolutionary feedback loop: Linking gene expression, trait evolution, and community dynamics. *Ecol. Lett.* 15: 492–501.
- Declerck, S. A. J. et al. 2015. Rapid adaptation of herbivore consumers to nutrient limitation: eco-evolutionary feedbacks to population demography and resource control. *Ecol. Lett.* 18: ed. by R. Sterner, 553–562.
- Del Giorgio, P. A. and Cole, J. J. 1998. Bacterial growth efficiency in natural aquatic systems. *Annu. Rev. Ecol. Syst.* 29: 503–541.
- Dumont, H. J. et al. 1975. The dry weight estimate of biomass in a selection of Cladocera, Copepoda and Rotifera from the plankton, periphyton and benthos of continental waters. *Oecologia* 19: 75–97.
- Fussmann, G. F. et al. 2000. Crossing the Hopf Bifurcation in a Live Predator-Prey System. *Science* 290: 1358–1360.
- Gaedke, U. et al. 2004. Biomass Size Spectra and Plankton Diversity in a Shallow Eutrophic Lake. *Int. Rev. Hydrobiol.* 89: 1–20.
- Humphreys, W. F. 1979. Production and respiration in animal populations. *J. Anim. Ecol.* 48: 427–453.
- Jensen, T. C. et al. 2006. Does excess carbon affect respiration of the rotifer *Brachionus calyciflorus* Pallas? *Freshw. Biol.* 51: 2320–2333.
- Morris, D. P. and Lewis, W. M. 1992. Nutrient limitation of bacterioplankton growth in Lake Dillon, Colorado. *Limnol. Oceanogr.* 37: 1179–1192.
- Rothhaupt, K. O. 1992. Stimulation of phosphorus-limited phytoplankton by bacterivorous flagellates in laboratory experiments. *Limnol. Oceanogr.* 37: 750–759.
- Rothhaupt, K. O. 1990a. Differences in particle size-dependent feeding efficiencies of closely related rotifer species. *Limnol. Oceanogr.* 35: 16–23.
- Rothhaupt, K. O. 1990b. Population growth rates of two closely related rotifer species: effects of food quantity, particle size, and nutritional quality. *Freshw. Biol.* 23: 561–570.
- Shertzer, K. W. and Ellner, S. P. 2002. State-dependent energy allocation in variable environments: Life history evolution of a rotifer. *Ecology* 83: 2181–2193.
- Straile, D. 1997. Gross growth efficiencies of protozoan and metazoan zooplankton and their dependence on food concentration, predator-prey weight ratio, and taxonomic group. *Limnol. Oceanogr.* 42: 1375–1385.
- Tittel, J. et al. 2012. Non-cooperative behaviour of bacteria prevents efficient phosphorus utilization of planktonic communities. *J. Plankton Res.* 34: 102–112.
- Vadstein, O. et al. 2003. Is phosphorus limitation of planktonic heterotrophic bacteria and accumulation of degradable DOC a normal phenomenon in phosphorus-limited systems? A microcosm study. *FEMS Microbiol. Ecol.* 46: 307–316.
- Vrede, K. et al. 2002. Elemental Composition (C, N, P) and Cell Volume of Exponentially Growing and Nutrient-Limited Bacterioplankton. *Appl. Environ. Microbiol.* 68: 2965–2971.
- Yoshida, T. et al. 2003. Rapid evolution drives ecological dynamics in a predator-prey system. *Nature* 424: 303–306.

Appendix 2 - Derivation of the exudation

We assume that the rate r_{growth} at which an alga grows in units of carbon is determined by a three-step process. First, organic carbon has to be fixed which happens at rate r_{fix} . Secondly a portion of this organic carbon is exudated at rate $e_{\text{dyn}} r_{\text{fix}}$. Finally the remaining carbon $(1 - e_{\text{dyn}}) r_{\text{fix}}$ may be used to build new biomass, depending on the nitrogen availability given by the Monod term $\frac{N}{H_A + N}$.

$$r_{\text{growth}} = (1 - e_{\text{dyn}}) r_{\text{fix}} \frac{N}{H_A + N} \quad (\text{S1})$$

The portion of organic carbon that is exudated increases under nitrogen limitation, given by $\left(1 - \frac{N}{H_A + N}\right)$. We assume that the exudation e_{dyn} is a linear function of the nitrogen limitation and bounded between a minimum e_{min} and a maximum e_{max} (Fig. S1a).

$$e_{\text{dyn}} = (e_{\text{max}} - e_{\text{min}}) \left(1 - \frac{N}{H_A + N}\right) + e_{\text{min}} \quad (\text{S2})$$

The flux of exudated carbon equals

$$r_{\text{exud}} = e_{\text{dyn}} r_{\text{fix}} \quad (\text{S3})$$

We assume that the production of organic carbon operates at a fixed rate. It is measured if nitrogen is not limiting, i.e. $\frac{N}{H_A + N} = 1$, as the maximum per capita growth rate in units of carbon and it follows from Eqs. S1 and S2 that

$$\begin{aligned} r_{\text{max growth}} &= \omega_{A,C} \beta_A \\ &= r_{\text{fix}} (1 - e_{\text{min}}) \end{aligned}$$

and therefore

$$r_{\text{fix}} = \frac{1}{1 - e_{\text{min}}} \omega_{A,C} \beta_A$$

With Eq. S3 the per capita exudation rate in unites of carbon becomes

$$r_{\text{exud}} = \frac{e_{\text{dyn}}}{1 - e_{\text{min}}} \omega_{A,C} \beta_A$$

The per capita growth rate under nitrogen limitation with exudation included (Eq. S1) thus becomes

$$\begin{aligned} r_{\text{growth}} &= \omega_{A,C} \beta_A \frac{1 - e_{\text{dyn}}}{1 - e_{\text{min}}} \frac{N}{H_A + N} \\ &= \omega_{A,C} F_A \end{aligned}$$

For plots of the exudation rate and growth rate at different maximal exudation ratios see Suppl. Fig. S1.

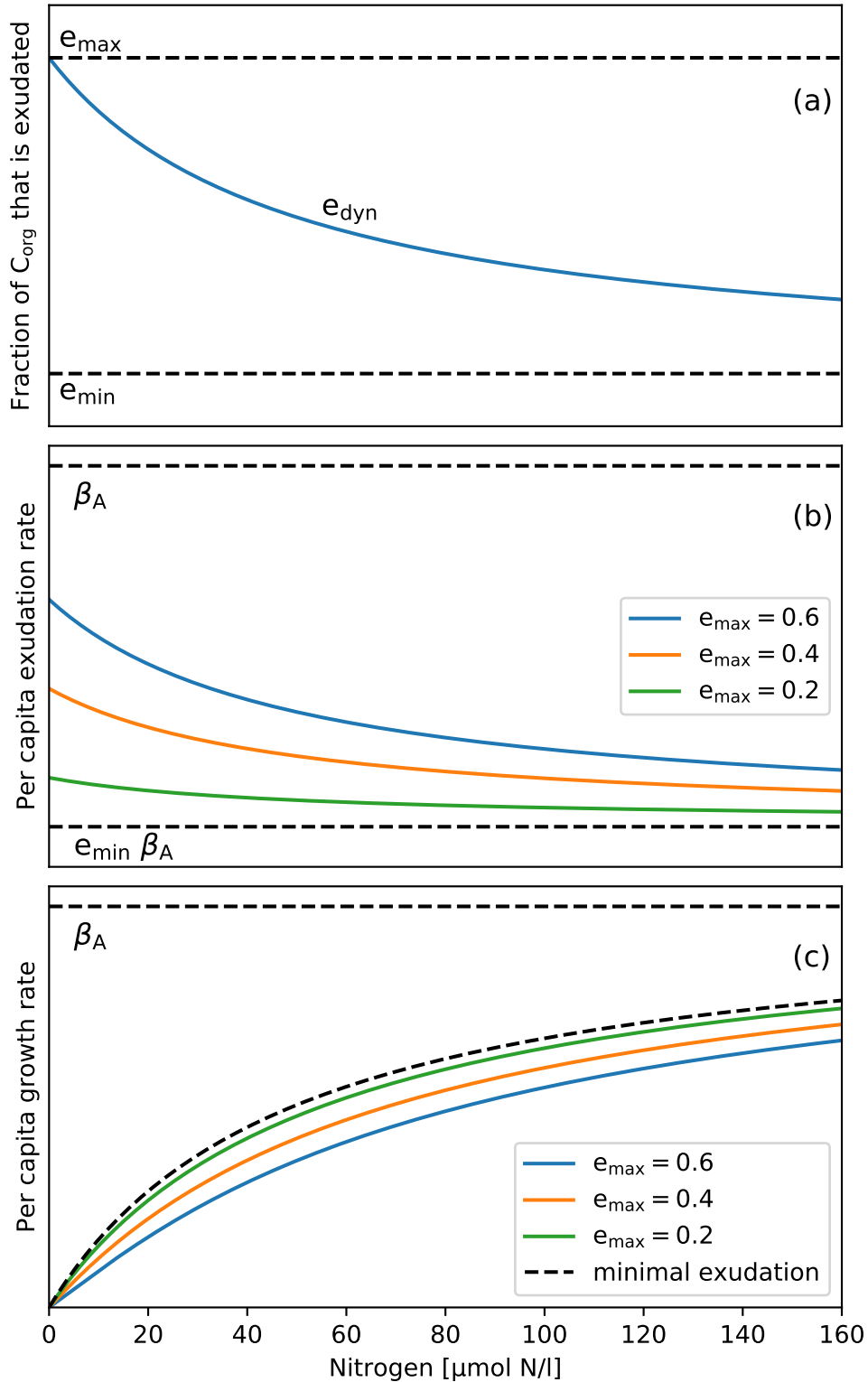


Figure S1 Effect of the exudation model for a half-saturation constant of $H_A = 49 \mu\text{molN/L}$ and a minimal exudation of $e_{\text{min}} = 0.1$. (a) Fraction of fixed carbon that is exudated. (b) Carbon exudation rate relative to the realized per-capita growth rate β_A . (c) Per capita growth rate. The dashed black line represents growth that is only affected by minimal exudation.

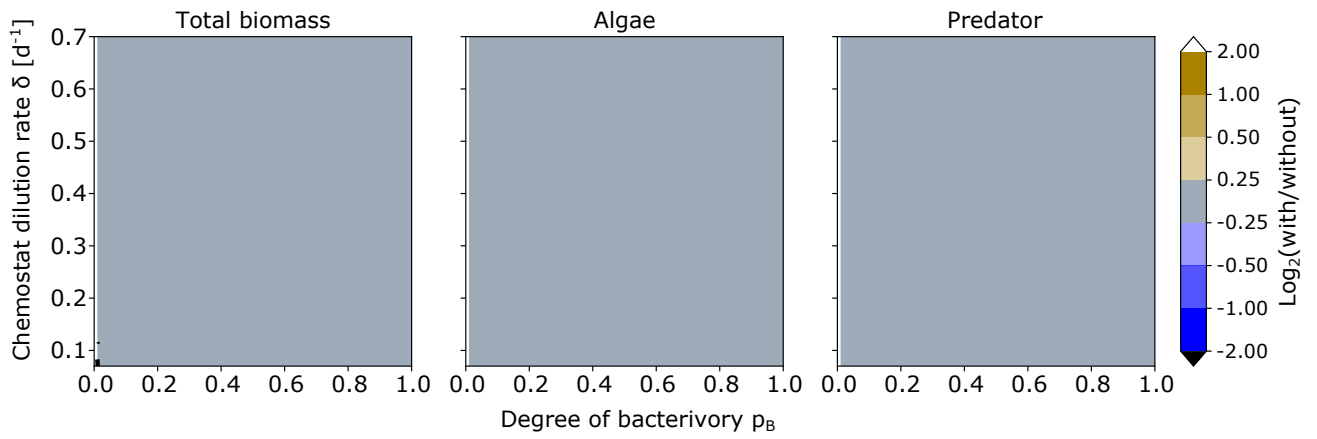


Figure S2 Effect size of bacterial presence under bacteria-suppressing conditions: $e_{\max} = 0.2$, $r_B = 0.7$ and $\varepsilon = 0.7$. The effect size is defined as the logarithmic ratio to base 2 of the mean biomasses with and without bacteria.

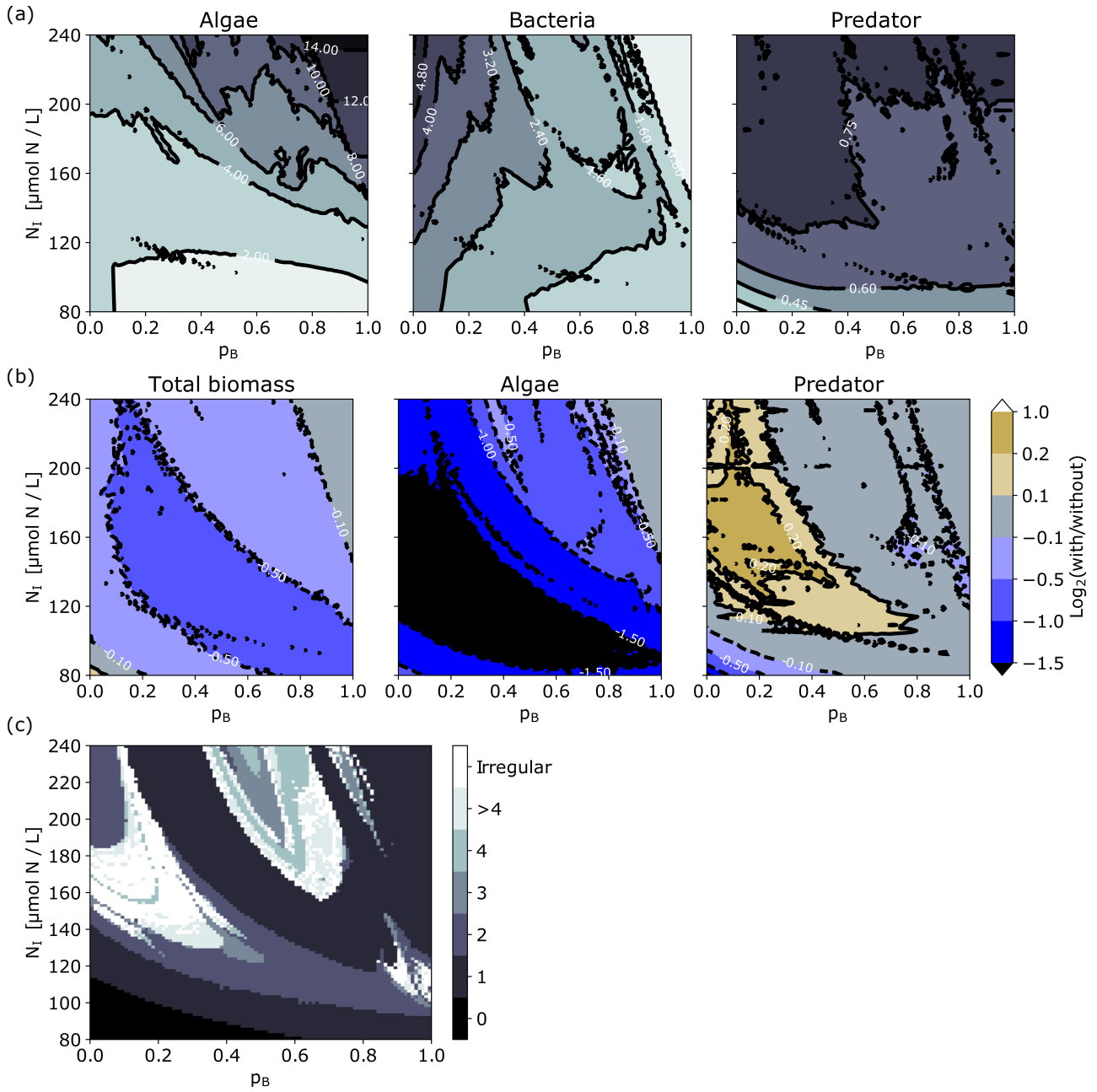


Figure S3 Parameter space spanned by degree of bacterivory p_B and nutrient inflow concentration N_I under favoring conditions at a dilution rate of $\delta = 0.35 \text{ d}^{-1}$ for (a) mean biomasses, (b) effect size of bacterial presence and (c) types of dynamics characterized by the number of algae maxima per repetitive unit.